

ICSV14

Cairns • Australia
9-12 July, 2007



EXPERIMENTAL STUDY OF THE FLOW-EXCITED ACOUSTICAL LOCK-IN IN A CORRUGATED PIPE

Vincent Debut^{1*}, José Antunes¹, Miguel Moreira²

¹Institute of Nuclear Technology, Applied Dynamics Laboratory, ITN/ADL - 2686
Sacavem codex, Portugal

²Polytechnic Institute of Setubal, Department of Mathematics, IPS/EST/DM - 2914-761
Setubal, Portugal

vincentdebut@itn.pt

Abstract

Preliminary experiments to study the aero-acoustic interaction in a corrugated pipe subjected to axial flow are reported. A number of pipes of different diameters, lengths and corrugation pitches and shapes are tested. Results are presented in the light of previous work and the aero-acoustic instability Strouhal numbers are evaluated. We notice that not a single value St is applicable for all tested tubes and discuss the qualitative differences observed.

1. INTRODUCTION

In the context of aerodynamic noise generation, flow-excited acoustic resonances can be encountered in a large variety of configurations, from engineering applications to musical acoustics and thus can be viewed as a source of noise problems or as an interesting sound source.

Here, the flow-acoustic phenomenon studied is that of sound generation in a corrugated tube in which air-flow interacts with the longitudinal acoustic modes of the pipe. In the literature, this configuration has been given less attention than other types of flow excited resonance. For instance, the case of a flow past a cavity or a cross-junction has been the subject of extensive studies [1, 2] and, to date, an important part of the underlying physics has been reasonably well understood. In our configuration - a kind of multi-shallow cavities system - the location of the source(s) is not as evident as in the latter configuration where the sound source is located at the separation point of the unstable flow. Nevertheless, Kristiansen and Wiik [3] presented recently interesting results centred on the study of the acoustical energy flow through corrugated pipes, with the objective to locate sound-producing regions.

The main purpose of this paper is to present experimental data and to compare it with the quantitative data found in the literature. Our objective is to identify the important parameters which control the relationship between the geometry of the system, the flow characteristics and the excited sound, focusing on the phenomenology observed.

2. EXPERIMENTAL SET-UP AND PROCEDURE

2.1. Test rig and instrumentation

The experimental set-up is shown in Figure 1. The working fluid is air, sucked through the corrugated tube by a quiet vacuum cleaner (residual noise in the range [55 - 90] dB for increasing velocity), which allows for mean flow velocity values between 0 to 40 m.s⁻¹ (for the largest pipe diameter). A settling chamber filled with foam insuring adequate isolation from the vacuum cleaner as well as open-end boundary conditions for the outlet end of the pipe, is lined with the tube which is placed on pipe supports. Flow velocities are adjusted with a suitable rheostat and are measured through a venturi tube inserted between the settling chamber and the vacuum cleaner. A *Velocical Plus meter* model 8386 measures the pressure drop Δp over the venturi tube (accuracy ± 1 Pa) and the average flow velocity through the venturi U_V is obtained from the Bernoulli equation $U_V = \sqrt{2\Delta p/\rho(1 - m^2)}$, with $m = 4$ the cross-section ratio of the cylindrical inlet and throat of the Venturi tube ($\rho = 1.2 \text{ kg.m}^{-3}$ is the density of air). The mean flow velocity in the corrugated tube U_0 is deduced using the conservation of mass from $U_0 = U_V S_i/S_{tube}$ where S_i and S_{tube} are respectively the cross-section of the venturi inlet and the corrugated pipe.

The acoustical pressure amplitude $p(t)$ and frequency f are measured at the open inlet of the tube by means of a sound level meters *Brüel & Kjaer* type 2221. Care was taken to put it into the same position and angle from the tube inlet for every tested tube (14 cm and 45°). The transmitter output is connected to the port of a *Spectral Dynamic* acquisition board (Model 20-42) which ensures the analog digital conversion.



Figure 1. Experimental set-up.



Figure 2. Sections of two tested corrugated tubes pipe 3 (up) and pipe 2 (down).

2.2. Processing of pressure signals

A PC computer and Siglab-VCAP software were used to acquire the time domain pressure signals. The sample frequency was fixed to 12.8 kHz and time-acquisition pressure signals were 10-second long. At each flow velocity, the pressure signal from the microphone was recorded and the power spectrum was calculated using Fast Fourier Transform algorithm. On the other hand, the Hilbert transform [4] was applied to the non-modified section of the windowed signal yielding the envelope and instantaneous frequency. Pressure level are normalized with the reference pressure $P_0 = 2.10^{-5}$ Pa.

Table 1. Dimensions of pipes used in experiments (mm - accuracy ± 0.05 mm).

	Pipe 1	Pipe 2	Pipe 3
Internal diameter, $D = 2R$	11.00	14.00	25.00
Corrugation pitch, p_c	3.20	3.40	4.20
Cavity depth, h_c	1.90	2.30	2.80
Cavity length, ℓ_c	0.90	1.10	1.95

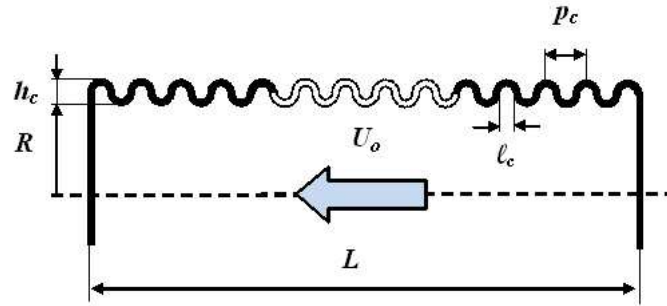


Figure 3. Definitions of the corrugation geometric parameters ℓ_c , p_c , h_c for a pipe of length L and radius R . U_0 is the mean flow velocity flowing through the pipe.

2.3. Investigated corrugated pipes

We tested a number of corrugated pipes with different diameters, lengths and corrugation distances. Typical dimensions are given in Table 1 (see Figure 3 for definitions). Lengths were $L = 0.5; 1; 2$ m. Wall shapes are quite similar for pipe 1 and 2 with the presence of rounded cavity edges; pipe 3 has sharper cavity edges (see Figure 2). Notice that because of their rounded corrugations shapes, the definition and measurements of the cavity length ℓ_c is delicate for pipe 1 and 2.

3. EXPERIMENTAL RESULTS

For a specific tube geometry, a given experimental run consists in step-increasing (resp. decreasing) gradually the flow velocity in the tube from zero (resp. maximum) to its maximum (resp. zero) value. Acquisitions were performed at each velocity step, after obtaining a steady response of the flow-acoustic system.

3.1. Preliminary observations

Figure 4 shows typical spectra for the sound pressure for two flow velocities. For low velocities most of the acoustic energy is confined at a single frequency of relative small amplitude and the tone is clear. At higher flow velocities, a fundamental frequency and its harmonically related components dominate clearly the spectrum. A broad-band noise “colored” by the passive resonances of the tube and corresponding to non-organized perturbations is also present. This affects the quality of the sound which is much more noisy. According to Pollack [5], these frequency peaks can be classified as *instability-generated tones* and *turbulent-generated tones* respectively.

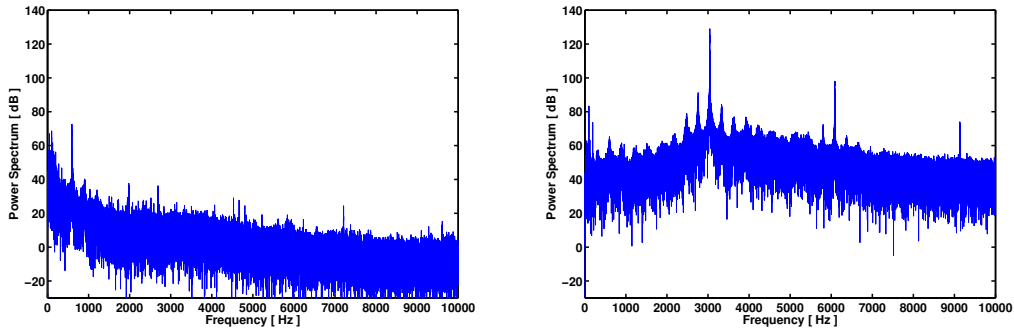


Figure 4. Power spectrum for two flow velocities. Pipe 3, $L = 0.5$ m. Right: $U_0 = 4.88$ m.s⁻¹, $f = 596$ Hz. Left: $U_0 = 31.50$ m.s⁻¹, $f = 3044$ Hz.

3.2. Evolution of the dominant oscillating frequency and amplitude with flow velocity

Around 100 pressure signals were acquired for each specific tube geometry. Representations of the evolution of the dominant frequency and pressure amplitude versus the mean flow velocity could then be plotted as well as spectrograms plots.

Figure 5 shows the general trend of the oscillating frequency of the system as the velocity is increased for a pipe with $D = 25$ mm and $L = 0.5$ m. We observed different stages corresponding to lock-in phenomena, each stage separated by discontinuous jumps in frequency and amplitudes. In all lock-in, oscillations are close to the normal modes of the pipes as it will be shown in Figure 7. Strickly speaking, we report oscillating frequencies 10% smaller than the resonance frequencies obtained from the usual equations for open-open smooth pipe. Nevertheless, these oscillating frequencies correspond to the resonance frequencies of the corrugated pipe and can be predicted more precisely using a formula derived by Cummings [6] which takes into account both effects of the corrugations and the mean flow. Finally, notice that the shape and characteristic of the curve in Figure 5 is very similar to that of the jet drive organ pipe as reported by Coltman [7].

Looking at the amplitude of the pressure spectrum in figure 5, we first observe that sound pressure levels are very high and that globally, the higher the resonance frequency, the higher the sound pressure is. For low flow velocities, it can be further noticed that within a specific lock-in stage, the sound pressure level increases, then passes through a maximum, and finally reduces suddenly as the flow velocity is increased (see also Figure 7). For high speed flow velocities, this trend is less marked.

Futhermore, the following points have been observed during our experiments:

- for all tested configurations, the fundamental mode never becomes unstable ;
- when the pulsation amplitude becomes large, the system exhibits hysteresis with flow velocity respectively when velocity is increased or decreased, a typical consequence of nonlinear effects (see Figure 10) ;
- although the system appears to behave in a reasonably systematic manner, modal jumps can sometimes behave unexpectedly (see Figure 10 for $U_0 \approx 37.8$ m.s⁻¹) ; we also notice that not all the harmonics are excited (for instance, absence of mode 19 in Figure 10) ;
- for the same corrugated pipe geometry (see Figure 6), the pressure amplitude appears to depend on the pipe length, the longer pipes being more noisy ; in such a case and for identical values of the flow velocity, the unstable oscillating frequency is the same ;

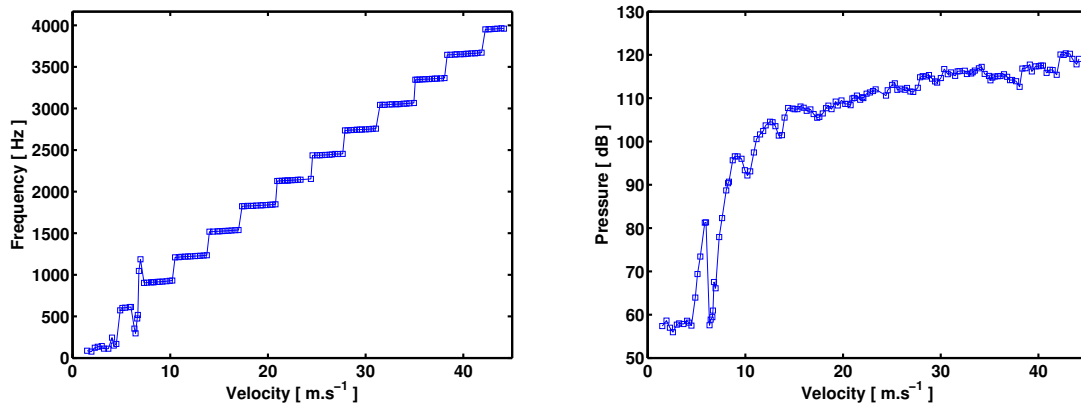


Figure 5. Evolution of the dominant frequency (left) and amplitude (right) versus mean flow velocity for pipe 3, $L = 0.5$ m.

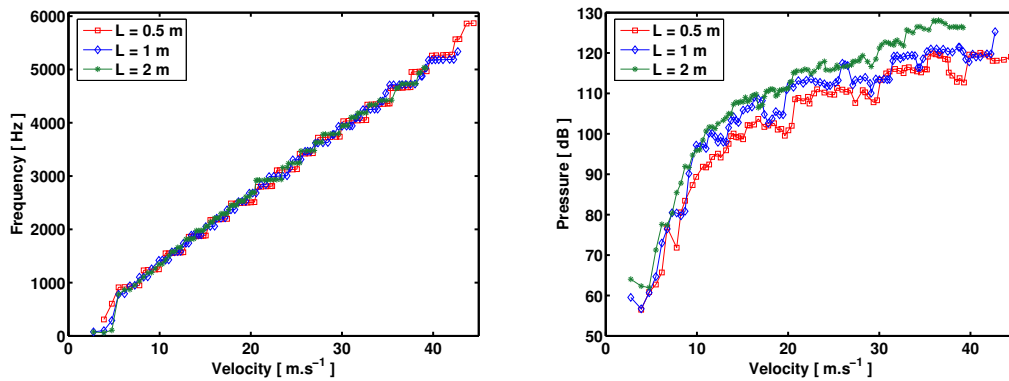


Figure 6. Evolution of the dominant frequency (left) and amplitude (right) versus mean flow velocity for different pipe lengths. Pipe 2.

- the shorter the tube, the wider is the lock-in velocity ranges. This is to relate to the modal density of the studied pipe ;
- multi-tones have been clearly identified between two locked-in stages. This can be viewed on the spectrogram in Figure 11 where overlapping are observed.

All these remarks suggest that the prediction of the system behaviour appears as a hard task.

3.3. Strouhal number

Referring to other flow induced acoustic resonance configurations such as annular restrictor in pipeline systems [8] or closed side branch systems [2], it is expected that the generation of self-sustained oscillations in a corrugated pipe is induced by a vortex shedding process with a phase relationship between the velocity disturbance and the acoustic oscillations. This phase is possibly determined by the time needed for a vortex to travel the distance between two corrugations i.e the corrugation pitch p_c . Tentatively, a Strouhal number St based on this geometric length has been defined as

$$St = \frac{f_v p_c}{U_0}, \quad (1)$$

where f_v is the vortex shedding frequency (which coincides with the dominant sounding frequency during lock-in) and U_0 is the mean flow velocity in the pipe. From our data, we obtain the Strouhal number given in Table 2 which are the mean values of the Strouhal number data

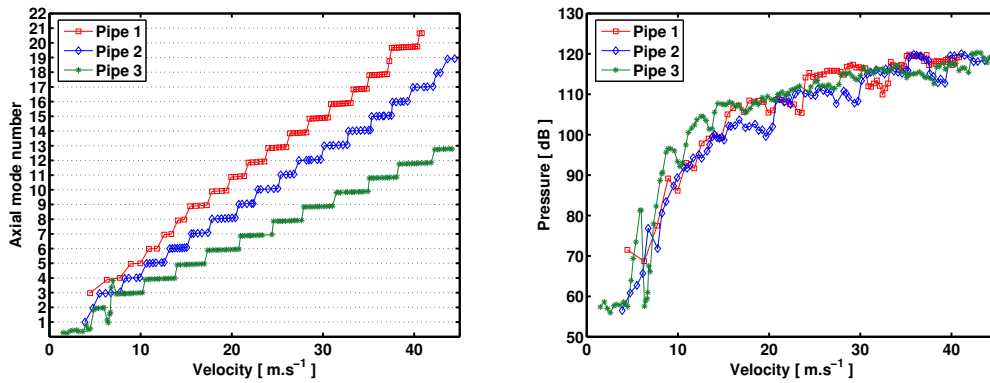


Figure 7. Axial mode number (left) and pressure amplitude (right) versus mean flow velocity for different pipe designs. $L = 0.5$ m. The reference fundamental frequency is $f_0 = 310$ Hz, obtained by acoustic measurements without flow, the pipe being excited by a loudspeaker.

over the velocity range $10 \text{ m.s}^{-1} < U_0 < 40 \text{ m.s}^{-1}$. First, Table 2 indicates that there is not a single value of St which is applicable for all corrugated pipe design, the identified Strouhal values ranging from 0.4 to 0.5. Then, our Strouhal number lie between the ones given in [3, 6, 9]. It can further be seen in Figure 8, deduced from Figure 7, that St decreases once the system is locked on a resonance mode and that there is also a general decrease as the flow velocity is increased. Unfortunately, since most of the tested results pertain to aero-acoustically unstable regimes, no linear law characteristic of purely fluid-dynamic vortex shedding could be detected in our measurements to confirm our Strouhal numbers as Nakamura and Fukamachi [9] did. An attempt in scaling our data to a reduced velocity has been done as shown Figure 9 but no simple relation has been found yet. Nevertheless, we believe that the phenomenon should be scaled by the corrugation pitch which is consistent with the characteristic length employed for the instability of a grazing flow along a resonator. From Table 2, we notice that Strouhal numbers are lower for the sharp edge corrugations pipe (pipe 3) than for the rounded edge corrugations (pipe 1 and 2). This is a striking analogy with the Strouhal numbers obtained for a square cylinder and circular cylinder which are $St \simeq 0.12$ and $St \simeq 0.2$ respectively [10]. Re-examining our results in the light of this remark, our differences in St , and thus the sound production mechanism, could be related to the precise geometry of the separation point of the vortex. This point should be investigated in detail by flow visualization.

3.4. Onset of the aero-acoustic instability

Crawford [11] suggested that the onset of an oscillating regime was correlated to the turbulence level in the pipe. Following this view, Cadwell [12] proposed a Reynolds number associated with the onset of turbulence ($Re \simeq 500$) but noticed that this is only true for long corrugated

Table 2. Identified Strouhal number for the studied pipe. Strouhal number are scaled to the corrugation pitch p_c and defined as $St = f_v p_c / U_0$. $\langle St \rangle$ is the mean values over the different pipe lengths. Notice that pipe 1 of length $L = 2$ m could not have been tested.

	$L = 0.5$ m	$L = 1$ m	$L = 2$ m	$\langle St \rangle$
Pipe 1	0.51	0.49	-	0.50
Pipe 2	0.44	0.44	0.45	0.44
Pipe 3	0.40	0.40	0.41	0.40

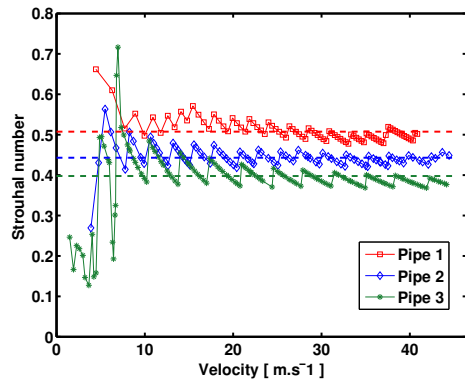


Figure 8. Determination of Strouhal number for pipes of length $L = 0.5$ m. Dotted lines correspond to the means value over $10 \text{ m.s}^{-1} < U_0 < 40 \text{ m.s}^{-1}$.

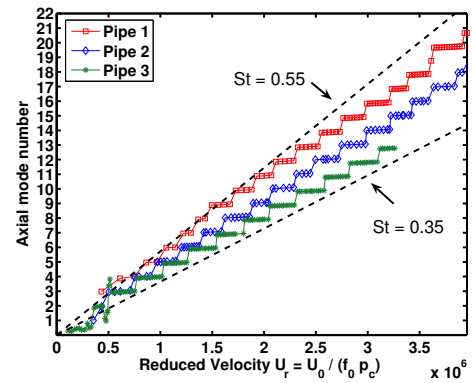


Figure 9. Evolution of the dominant frequency versus reduced velocity $U_r = U_0 / (p_c f_0) \cdot L = 0.5$ m. f_0 is the pipe fundamental modal frequency.

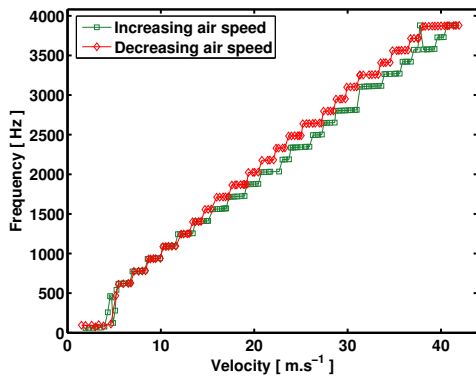


Figure 10. Evolution of the oscillating frequency as a function of flow velocity. Pipe 3, $L = 1$ m. Notice that oscillation jump occurs with hysteresis.

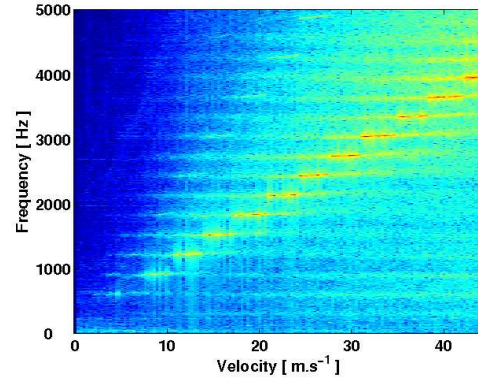


Figure 11. Spectrogram for a flow velocity sweep. Pipe 3, $L = 0.5$ m. Notice the presence of overlapping between lock-in stages which could results in multi-tones.

pipes. Observations of Petrie and Huntley [13], then confirmed by Elliot [6] and Kristiansen and Wiik [3], lead to the conclusion that the onset of oscillation is strongly influence by the shear layer instability at the pipe entrance. We also confirm that such is the case in our experiments. This does suggest that one should examine in detail the boundary layer at the entrance.

3.5. Physical mechanism of sound generation

Concerning the coupling mechanism, both the presence of different regimes of oscillation and the small deviation of the oscillating frequency of the system in a given range of velocity are typical observations of frequency lock-in phenomenon, as defined by de Langre [14]. Furthermore, the presence of a drastic increase in the oscillating pressure amplitude (between [10-40] dB depending on the flow velocity) shows that the mechanism is with an acoustic feedback which sustains the oscillation. Below the critical minimum velocity, the hydrodynamic perturbations due to the corrugations decay to brandnoise turbulence ; on reaching the minimum instability velocity boundary, the perturbations within the shear layer are amplified by the acoustical resonance effects resulting in strong oscillations. Measurements of Nakamura and Fukamachi [9] of the vortex shedding frequency outside the region of lock-in reinforce this statement.

4. CONCLUSIONS

A set of extensive experiments was performed to collect reliable data in order to examine the nature of the aero-acoustic interaction in corrugated pipes. These experiments confirm most of the observed qualitative behaviour reported in the literature but also show that many features observed are not easy to explain. Before any further conclusions can be reached as to the nature of the interaction between flow and acoustic, it will be helpful to obtain a dimensionless representation of these data. To date, no simple scaling relation has been found. Furthermore, a global observation of the obtained Strouhal number has shown that the sharpness of the corrugations must be considered when studying the onset of the instability. Flow visualizations will then be of great help in understanding the phenomena involved in the sound generation process.

Acknowledgements

This work was supported financially by the Portuguese Foundation of Sciences and Technology (*Fundação para a Ciência e a Tecnologia*). The authors would also like to thank Professor J. Fitzpatrick from Trinity College for fruitful advises.

REFERENCES

- [1] P. A. Nelson, N. A. Halliwell, and P. E. Doak. Fluid dynamics of a flow excited resonance, part II: flow acoustic interaction. *J. Sound and Vib.*, 91:375–402, 1983.
- [2] S. Dequand, S. J. Hulshoff, and A. Hirschberg. Self-sustained oscillations in a closed side branch system. *J. Sound and Vib.*, 265:359–386, 2003.
- [3] U. R. Kristiansen and G. A. Wiik. Experiments on sound generation in corrugated pipes with flow. *J. Acoust. Soc. Am.*, 121(3):1337–1344, 2007.
- [4] A.V. Oppenheim and R.W. Schaffer. *Discrete-Time Signal Processing*. Prentice-Hall.
- [5] M. L. Pollack. Flow-induced in side-branch pipe resonators. *J. Acoust. Soc. Am.*, 67(4):1153–1156, 1980.
- [6] J. W. Elliot. *Lectures Notes on the Mathematics of Acoustics*. Wright M.C.M, 2005.
- [7] J. W. Coltman. Jet drive mechanisms in edge tones and organ pipes. *J. Acoust. Soc. Am.*, 60(3):725–733, 1976.
- [8] A. K. Stubos, C. Benocci, E. Palli, Stoubos G. K, and D. Olivari. Aerodynamically generated acoustic resonance in a pipe with annular flow restrictor. *J. Fluids and Struct.*, 13:755–778, 1999.
- [9] Y. Nakamura and N. Fukamachi. Sound generation in corrugated tubes. *Fluids Dynamics Research*, 7:255–261, 1990.
- [10] R. D. Blevins. *Applied fluid dynamics handbook*. Van Nostrand Reinhold, 1984.
- [11] F. S. Crawford. Singing corrugated pipes. *Am. J. Phys.*, 62:278–288, 1974.
- [12] L. H. Cadwell. Singing corrugated pipes revisited. *Am. J. Phys.*, 62:224–227, 1994.
- [13] A. M. Petrie and I. D. Huntley. The acoustic output produced by a steady airflow through a corrugated duct. *J. Sound and Vib.*, 70:1–9, 1980.
- [14] E. de Langre. Frequency lock-in is caused by coupled-mode flutter. *J. Sound and Vib.*, 265:359–386, 2006.